Hindawi
Journal of Advanced Transportation
Volume 2024, Article ID 1783038, 17 pages
https://doi.org/10.1155/2024/1783038

Research Article

A Multiscale Approach for Free-Float Bike-Sharing Electronic Fence Location Planning: A Case Study of Shenzhen City

Zhonghua Wei, Houqiang Ma, and Yunxuan Li

Beijing Key Laboratory of Traffic Engineering, College of Metropolitan Transportation, Beijing University of Technology, Beijing, China

Correspondence should be addressed to Yunxuan Li; liyunxuan_1989@163.com

Received 30 July 2023; Revised 30 January 2024; Accepted 13 February 2024; Published 28 February 2024

Academic Editor: Jinjun Tang

As an emerging technological means for managing free-float bike-sharing parking, electronic fences have attracted increasing attention in major cities as a solution to the challenges posed by disorderly parking of free-float bikes. Existing research has predominantly focused on employing clustering methods from the perspectives of free-float bike-sharing companies and users to plan and deploy electronic fences. However, the results often deviate significantly from the actual phenomenon. Therefore, scientific location selection is particularly important to fully harness the effectiveness of electronic fences. This paper proposes a multiscale clustering method based on free-float bike-sharing parking features to determine the optimal locations for electronic fences. A multiobjective mixed-integer programming model is established to address the location planning problem of electronic fences, determining the planning positions, quantities, and areas of electronic fences. A case study is conducted using a local area free-float bike-sharing dataset from Shenzhen city to validate the effectiveness of the proposed method. Comparative results with traditional approaches solely relying on *K*-means or DBSCAN methods demonstrate that the proposed approach achieves efficient location selection, through multiscale fusion site selection in the study area of 1.5 $*$ 1 km, and only 25 electronic fences need to be planned and deployed, covering a total area of 1691.88 square meters, which can provide rational placement solutions and better utilize the effectiveness of electronic fences. This method can thus offer decision-making support for the planning and location selection of electronic fences in free-float bike-sharing systems.

1. Introduction

Under the multiple drivers of "green," "sharing," and "Internet+," free-float bike-sharing has emerged as a new mode of transportation, providing efficient and environmentally friendly travel services to urban residents. They contribute to reducing greenhouse gas emissions, alleviating urban traffic congestion, improving urban mobility, and serving as an effective means of transportation for the "last mile" in cities. As of 2023, there are over 2,000 operational free-float bike-sharing systems worldwide. The notable free-float bike-sharing companies include Lime, Bird, Jump, and Spin in the United States, Swapfiets and Donkey Republic in the Netherlands, and Donkey Republic and GoBike in Denmark. In China, companies such as Hellobike and Mobike have made significant contributions to the growth of free-float bike-sharing. China became the largest free-float bike-sharing market in the world in 2020, covering over 360 cities, with an average daily ridership of 47 million trips [1]. The user base has also expanded, growing from 220 million people in 2017 to 300 million people in 2021.

However, the explosive growth in the number of free-float bike-sharing has posed new challenges to urban public management. The haphazard and disorderly parking of bicycles not only occupies public resources (e.g., motor vehicle lanes, auxiliary lanes, and tactile pavements) but also disrupts traffic order (e.g., blocking subway exits and bus platforms) and affects the city's aesthetics. It damages the user's experience and even hampers the sustainable development of urban transportation [2, 3]. According to the "2017 Special Report on China's Summer Free-Float Bike-Sharing Market," 42% of users considered the problem of

disorderly parking of free-float bike-sharing to be severe, while 26.8% considered it to be extremely severe [4]. Moreover, the demand for free-float bike-sharing exhibits spatiotemporal heterogeneity, with pronounced tidal phenomena [5–8].

Against this backdrop, the "free-float bike-sharing electronic fence" has emerged as a primary means of managing free-float bike-sharing parking. Based on "Bluetooth beacon" technology, the electronic fence utilizes information technology to define virtual parking stations, dividing parking areas into operational and nonoperational zones and regulating parking and no-parking areas. Users are guided via mobile apps to designated locations for bike borrowing and return, thereby enforcing orderly parking behavior. Although electronic fences have been implemented in some cities, they still face several challenges such as follows: (1) there is a lack of interaction between electronic fences and free-float bike-sharing data, leading to improper location selection. Some electronic fences may have no available bikes for borrowing, while others may have no available parking spots for returns; (2) an excessive number of electronic fences may lead to suboptimal effects before and after their implementation, and the problem of arbitrary parking can still be observed; and (3) there may be a mismatch between the size of electronic fences and the demand. Some areas may have excessively large electronic fences, resulting in wasted public land resources and chaotic and disorderly parking of free-float bike-sharing. Conversely, some areas may have inadequate space, preventing users from returning bikes. Therefore, the rational planning and deployment of electronic fences in terms of location, quantity, and size pose significant challenges to the development of free-float bike-sharing.

Free-float bike-sharing, as a successful application of the Internet of Things (IoT), generates a vast amount of data with spatial and temporal tags. In the planning and deployment of electronic fences, researchers often rely on unsupervised machine learning clustering methods based on the data tags [9, 10], of which the most commonly used methods include *K*-means clustering [11] and DBSCAN [12]. Some scholars have also developed location-allocation models (such as the p-median, p-center, and maximum coverage problem models) [13, 14], considering the perspectives of free-float bike-sharing companies and users when planning the deployment of electronic fences. However, using a single clustering analysis method alone can lead to rough results with strong randomness due to the uneven distribution density of free-float bike-sharing. In the planning and deployment of electronic fences, it is also necessary to consider maintaining the city's aesthetics and appearance to ensure the sustainable development of free-float bike-sharing.

The research is based on the large-scale data of free-float bike-sharing orders, proposing a multiscale clustering fine-grained exploration method based on the spatial distribution characteristics of free-float bike-sharing to determine candidate locations for planning electronic fences for free-float bike-sharing. From the perspectives of users, enterprises, and urban management, a comprehensive consideration is given to the rational selection of electronic fence locations, determining the positions, quantities, and areas where electronic fences for free-float bike-sharing should be deployed within the designated region.

The remainder of the paper is structured as follows. Section 2 presents a review of the spatial and temporal characteristics of bicycle sharing and studies related to bicycle sharing site planning. Section 3 presents the problem description and the model formulation. Section 4 presents a case study of the Shenzhen city bike-sharing dataset. Section 5 presents discussion with limitations and future work.

2. Literature Review

The analysis of spatiotemporal characteristics of free-float bike-sharing is fundamental for the planning and deployment of electronic fences. Numerous scholars have conducted relevant research on the spatiotemporal distribution characteristics of free-float bike-sharing origin-destination (OD) patterns. In terms of temporal characteristics, scholars have mostly used bar or line graphs to visualize the amount of free-float bike-sharing usage per unit time period [15, 16]; in terms of spatial characteristics, scholars have mostly used grid cell statistical analysis, kernel density analysis, and point-of-interest distribution analysis [17–19]. Compared with the traditional siting of public bicycles with stakes, the site of electronic fences for free-float bike-sharing is more inexperienced. The location, quantity, and area of the electronic fence are all factors to be considered, and the bike has the characteristics of random parking and the tidal phenomenon is more prominent, which makes the siting of the electronic fence more complicated. At present, the site selection problem mainly focuses on the layout planning research, and scholars mostly construct mathematical model algorithms and determine the site selection plan with the help of geographic information software and other methods.

Reasonable planning and deployment of electronic fences can enhance the efficiency and user satisfaction of free-floating bike sharing, thereby playing a crucial role in promoting urban transportation development. Various mathematical models and algorithms have been widely used in this area. Zhang et al. [20] employed the maximum coverage method to plan the deployment of electronic fences for free-float bike-sharing in Shanghai, and the results showed that with 7500 fences, 91.8% of parking demands could be covered. Guo et al. [21] developed a mixed-integer optimization model to optimize the layout of free-float bike-sharing parking lots on a campus, considering travel time and cost as optimization objectives. The optimization results demonstrated a 6.0% reduction in average travel time and a 27.3% decrease in construction costs. García-Palomares [22] conducted a comparative analysis of the maximum coverage model and the p-median model to evaluate the rationality of site selection for bike stations, and the results indicated that the maximum coverage model yielded more significant outcomes. Martinez et al. [23] established an

integer linear programming model with the objectives of minimizing costs and maximizing coverage range and solved the model accordingly. Wang et al. [24] utilized the DBSCAN algorithm to cluster the pickup locations of bicycles, grouping 432 bikes into 12 clusters. Mahmoodian et al. [25] performed clustering analysis on free-float bike-sharing data using an integer programming model, *K*-means algorithm, and DBSCAN algorithm. They compared the distances from users to cluster virtual stations and the time required by different clustering methods, ultimately selecting the *K*-means clustering method. Caggiani et al. [9] employed a space-time clustering method to select virtual stations within a 500 m ∗ 500 m grid. Hua et al. [10] compared *K*-means clustering, DBSCAN clustering, and a 50 m ∗ 50 m grid approach for selecting virtual bike stations. Yang and Chen et al. [26, 27] developed a coverage model considering both spatial and temporal aspects, aiming to maximize the spatiotemporal demand while minimizing the distance between users and bike stations. Hu et al. [28] applied the maximum coverage problem to optimize and evaluate a free-float bike-sharing project in Boulder, Colorado, providing three strategies for improving the free-float bike-sharing system. Park et al. [13] employed two different location-allocation models and found that the sites determined by the p-median were dispersed throughout the area, while those determined by the MCLP model were more concentrated in the central region. Frade et al. [14] considered the construction cost of free-float bike-sharing stations and, under a fixed budget, used the MCLP model to determine suitable locations for station planning and deployment. Guo et al. [29] simultaneously considered macrolevels and microlevels, adopting DBSCAN and mixed-integer linear programming for site selection and capacity determination at the macrolevel and employing a traffic flow simulation to establish an agent-based model for microlevel parking layout planning. It can be observed that domestic and foreign scholars have conducted some research studies on bike-sharing site selection, mainly through unsupervised machine learning clustering perspective (DBSCAN and K-means) and established mathematical models from the perspective of users and enterprises.

In the field of geographic information systems (GISs), Kabak et al. [30] combined different multicriteria decision-making methods with GIS to determine indicator weights and analyze the suitability of free-float bike-sharing station locations. Conrow et al. [31] utilized spatial analysis (GIS and spatial optimization) and coverage models to help establish free-float bike-sharing stations throughout the city, thereby reducing the distance users need to travel. Nyimbili and Erden [32] described the uncertainty of user travel and conducted spatial analysis of free-float bike-sharing stations by combining fuzzy GIS analysis with the analytic hierarchy process (AHP). Banerjee et al. [33] assumed a correlation between potential free-floating bike sharing station locations and roadway use intensity, improved the gravity model, and used GIS to assess the suitability of free-floating bike sharing station locations. Yang et al. [34, 35] proposed a shared parking space allocation model and a timed shared parking space allocation model to improve the utilization efficiency of parking in residential communities. Fu et al. [36] proposed a new integrated site selection model for bike-sharing stations with the aim of maximizing daily revenue for a given station location and total investment in bike acquisition. In addition, scholars optimized the operation strategies of the bike-sharing system, including minimizing the division time in balanced scheduling operation [37] and minimizing carbon dioxide emissions [38].

In summary, a proper and well-planned deployment of electronic fences is essential for ensuring the sustainable and healthy development of the free-float bike-sharing. It helps improve the free-float bike-sharing system and holds significant significance and value. Currently, the selection of electronic fence locations often relies on clustering analysis methods, but the clustering results may lack granularity and precision. In addition, in the construction of location selection models, the focus is primarily on user and enterprise perspectives, while factors related to urban public management are often not adequately considered. This paper proposes a multiscale and fine-grained clustering method that leverages the distribution characteristics of free-float bike-sharing location big data. It considers the strengths and weaknesses of *K*-means and DBSCAN, using a layered approach that applies DBSCAN clustering on top of the initial *K*-means clustering to extract candidate locations for electronic fence deployment at a finer granularity. The proposed method considers the perspectives of urban management, enterprise, and users to rationally plan and deploy free-float bike-sharing electronic fences.

3. Materials and Methods

3.1. Select Candidate Site for Free-Float Bike-Sharing Electronic Fences. Based on the spatiotemporal big data of free-float bike-sharing, unsupervised learning methods such as *K*-means and DBSCAN clustering are commonly employed to extract hotspots such as free-float bike-sharing stations. *K*-means clustering is based on the similarity measure, which groups samples with similar distances into the same subset, minimizing the differences between elements in the same subset. It assumes strong convexity of the dataset, has low time complexity, and requires a specified number of clusters. On the other hand, DBSCAN is a density-based clustering algorithm that can automatically identify the number of clusters and handle irregularly shaped clusters as well as outliers. It requires defining a neighborhood radius and minimum density to partition data points and gather density-reachable points into the same cluster. DBSCAN has a higher time complexity, making it inconvenient for large data processing. However, the distribution of free-float bike-sharing parking spots is irregular and often exhibits block-

like, strip-like, and scattered patterns. *K*-means does not handle these situations well. DBSCAN can compensate for the limitations of *K*-means as it can automatically identify irregularly shaped clusters and exhibits good robustness to outliers. However, since the density of free-float bike-sharing parking big data varies spatially, using the same parameters directly does not yield satisfactory results, and the computational complexity is high, leading to long processing times.

Considering the distribution characteristics, outliers, and time complexity of free-float bike-sharing, with reference to the advantages and disadvantages of the above-mentioned two algorithms, this section adopts a superimposed fusion approach to select electronic fences using a multiscale fine-grained clustering method. First, considering the differences between categories, the *K*-means algorithm is used at the macrolevel to cluster the large dataset of free-float bike-sharing, and classifying regions according to the spatial distribution characteristics of free-float bike-sharing divides a large number of data points into fewer clusters, which reduces the complexity of the data and serves to downscale the data, making it easier to understand and analyze. Then, based on the *K*-means clustering results, the DBSCAN clustering is performed by specifically adjusting the parameters of each class according to the characteristics of the distribution of bicycles in each class, and in order to reduce the false detections and to better adapt to the situation of uneven data density, the direct use of the same DBSCAN radius may not be able to capture this difference well, and the global radius setting may lead to excessive clustering or missed detections because it is not sensitive to the characteristics of the different clusters, and by choosing the appropriate radius for each cluster, it is possible to reduce the false detections, so as to improve the accuracy of the site detection and to better capture the characteristics of the distribution of the clusters in the different regions, which will lead to a more targeted site selection.

The within-cluster sum of squares (WCSS), silhouette coefficient, and Calinski–Harabasz index (CH index) are used to evaluate the clustering performance. Algorithm 1 demonstrates a complete algorithm for multiscale hierarchical clustering based on free-floating bicycle sharing big data. At the macrolevel, the inputs are the free-floating bicycle sharing dataset, the number of clusters "k_values," the radius of the neighborhood "eps_values," and the minimum number of data points "min_p"; by evaluating the metrics "WCSS" and "Silhouette coefficients," it will output the number of best clusters "best_k" and the macroclustering results. At the microlevel, based on the macroclustering results, the best neighborhood radius "best_eps(idx)" of each class is obtained through the evaluation of indicators such as "Silhouette coefficient" and "CH index"; the parking characteristics of free-float bike sharing are more fully taken into account, which leads to accurate and reasonable selection of the location of the electronic fence.

3.2. Model Formulation. The planning and deployment of electronic fences for free-float bike-sharing will inevitably have an impact on users, businesses, and urban management. For users, the deployment of electronic fences increases the walking distance to their destinations. For businesses, the development of electronic fence technology and the allocation of land require cost investment. For urban public management, the deployment of electronic fences will have an impact on the city's appearance and traffic order. Therefore, it is necessary to balance the relationships among these factors, and it is worth exploring the reasonable planning of the location, area, and capacity of electronic fences for free-float bike-sharing.

3.2.1. Model Assumptions

(1) Users can use a mobile app to access information about nearby electronic fence locations and choose the nearest one to borrow or return free-float bike-sharing.

(2) There are multiple user demand points and electronic fence locations. Each electronic fence can serve multiple user demand points, but each demand point can only choose one electronic fence for free-float bike-sharing borrowing or return.

(3) Users are only allowed to borrow or return free-float bike-sharing within the designated electronic fences.

(4) This study uses the Euclidean distance instead of street distance. Most of the bicycle systems studied are based on urban areas, which typically have a high density of roads and intersections. This allows people to make journeys in any direction by using the road, with the distance traveled unlikely to be far beyond the straight-line or Euclidean distance. In addition, the bike user is less likely to take long detours than other transport users (such as car drivers and metro riders) who are more constrained within their road network in the urban area. For this reason, O'Brien et al. [39] indicated that an Euclidean distance simplification in the bike system is more likely to be valid for urban areas, with a higher road and intersection density.

```
input: dataset, k_values, eps_values = [10, 25], min_p = 10
output: best_k, macro_clusters, best_eps (idx), micro_clusters
  for k = k_values
      kmeans = fitckmeans (dataset, k)
      labels = predict (kmeans, dataset)
      evaluation indicator = [WCSS, Silhouette coefficient]
  end
    best_k = k_values(best_k_idx)//choose the best k value
    kmeans = fitckmeans(data, best_k)//k-means macroclustering
    micro_clusters = cell (best_k, 1)
  for cluster_label = 1 : best_k
      for eps = eps_values
        dbscan_labels = dbscan(cluster_data, eps, 10)
        evaluation indicator = [ WCSS, Silhouette coefficient, CH index]
    end
      best_eps = eps_values(best_eps_idx)//choose the best eps value
      dbscan_labels = dbscan(cluster_data, best_eps, 10)//dbscan microclustering
      micro_clusters{cluster_label} = dbscan_labels;
    end
```

Algorithm 1: The multiscale clustering.

3.2.2. Notation. The symbols used in this model are shown in Table 1.

3.2.3. Formulation

$$
\begin{aligned}
&\text{Min } Z_1 = C_1 \sum_{j\in J} Y_j + C_2 \sum_{j\in J} V_j Y_j,\\
&\text{Min } Z_2 = C_2 \left(\sum_{k\in K} \sum_{j\in J} X_{kj} l_{kj} q_k + \sum_{i\in I} \sum_{j\in J} X'_{ij} l_{ij} q_i \right),\\
&\text{Max } Z_3 = -\sum_{j\in J} P(j) \log_2 P(j),\\
&\text{S.t.}\\
&\quad X_{kj} \le Y_j, \quad \forall k \in K, j \in J,\\
&\quad X'_{ij} \le Y_j, \quad \forall i \in I, j \in J,\\
&\quad \sum_{j\in J} X_{kj} = 1, \quad \forall k \in K,\\
&\quad \sum_{j\in J} X'_{ij} = 1, \quad \forall i \in I,\\
&\quad V_j = \frac{\left(q_{j0} + \sum_{i\in I} X'_{ij} q_i - \sum_{k\in K} X_{kj} q_k\right) \alpha \coprod \left(Y_j = 1\right)}{\beta}, \quad \forall j \in J,\\
&\quad \begin{cases} l_{kj} <= \mathrm{l}_{\max}, & \forall k \in K,\\ l_{ij} <= \mathrm{l}_{\max}, & \forall i \in I, \end{cases}\\
&\quad P(j) = \frac{V_j}{S},\\
&\quad \sum_{j\in J} Y_j \le n,\\
&\quad Y_j = \{0, 1\}\ X_{kj} = \{0, 1\}\ X'_{ij} = \{0, 1\}.
\end{aligned}
\tag{1}
$$

In the abovementioned model, the objective function 1 is the enterprise cost, which is composed of the construction cost and the land use cost of the electronic fence; the objective function 2 is the user satisfaction, which is composed of the user borrowing distance and the returning distance, and the smaller the distance, the higher the user satisfaction; the objective function 3 is the electronic fence spatial entropy, which measures the uncertainty or irregularity degree of the electronic fence distribution in a region, and a smaller electronic fence spatial entropy indicates that the electronic fence is more concentrated and evenly distributed, which can make the visual feeling of the city more neat and orderly and reduce the sense of clutter.

Constraints 4 and 5 indicate that the electronic fence must be in the open state when the demand point is served; constraints 6 and 7 indicate that the demand for borrowing and returning bikes can only be satisfied by one electronic fence; constraint 8 indicates the calculated area for e-fence deployment, which consists of the initial capacity, the number of returned bikes, and the number of borrowed bikes; constraint 9 indicates that the walking distance for users to borrow and return bikes is less than the maximum walking distance; constraint 10 indicates the percentage of each bike in the study area; constraint 11 indicates that the selected number of electronic fence cannot exceed the number of candidate electronic fence; constraint 12 indicates that the three decision variables are 0 and 1 variables.

3.2.4. Grey Relational Analysis. Based on the Pareto optimal solution generated by the abovementioned multiobjective optimization problem, in order to objectively and quantitatively evaluate the Pareto solution set to rank and select the optimal site selection solution from the Pareto solution set, this paper proposes the use of grey relational analysis (GRA). The steps are as follows.

Table 1: Notations of model formulation.

Sets	Definition
J	Electronic fence candidate collection, $J = \{1, 2, \ldots, j\}$
K	Collection of user demand points for borrowing bikes, $K = \{1, 2, \ldots, k\}$
I	Collection of user demand points for returning bikes, $I = \{1, 2, \ldots, i\}$
Variables	
Y_j	Equals 1 if the electronic fence is deployed in the location j, 0 if not
X_{kj}	Equals 1 if the demand for borrowing bike point k is served by electronic fence j, 0 if not
X_{ij}	Equals 1 if the demand for returning bike point k is served by electronic fence j, 0 if not
V_j	The area for planning and deployment of electronic fence j. Unit: m^2
Parameters	
q_{j0}	The number of initial bikes at the electronic fence j
q_k	User demand for borrowing bikes at k
q_i	User demand for returning bikes at i
$C_1C_2C_3$	Fixed cost of electronic fence, unit: yuan/place; the cost of land occupation for bikes. Unit: yuan/m^2; the distance cost incurred during the process of bike borrowing and returning by users, yuan/m
$P(j)$	Percentage of area per electronic fence j in the study area
α	The land area occupied by each individual bicycle, m^2/vehicle
n	Number of candidate electronic fences
β	Electronic fence capacity coefficient
$l_{kj}l'_{ij}l_{\max}$	The distance generated by the user during the borrowing process; the distance generated by the user during the returning process; the maximum distance of borrowing and returning bikes

Step 1. Determine the comparison sequence and reference sequence

Assuming that there are m programs and n evaluation indicators, a comparison sequence of $m * n$ can be constructed, where the m th program comparison sequence is denoted as

$$X_{mn} = \{x_{m1}, x_{mw}, \ldots, x_{mn}\}. \tag{2}$$

The reference sequence is the desired standard sequence used for comparison, which is denoted as

$$X_{0n} = \{x_{01}, x_{0w}, \ldots, x_{0n}\}. \tag{3}$$

Step 2. Normalized processing

To eliminate the effect of each indicator measure, the series was normalized and noted as

$$x'_{mn} = \frac{x_{mn}}{1/m\sum_1^m x_{mn}}. \tag{4}$$

Step 3. Calculate the number of correlation coefficients

The correlation coefficient ξ_{mn} for the nth indicator of the m th program is denoted as

$$\xi_{mn} = \frac{\min_m \min_n \left|x'_{0n} - x'_{mn}\right| + \rho \max_m \max_n \left|x'_{on} - x'_{mn}\right|}{\left|x'_{0n} - x'_{mn}\right| + \rho \max_m \max_n \left|x'_{on} - x'_{mn}\right|}. \tag{5}$$

Step 4. Calculate the grey correlation degree

Calculate the gray correlation of each scheme, the larger the value represents the stronger the correlation between the scheme and the objective, and select the scheme with the maximum gray correlation as the optimal scheme. The gray correlation calculation formula is denoted as follows:

$$R_m = \frac{1}{n}\sum_1^n \xi_{mn}. \tag{6}$$

4. An Illustrative Analysis

4.1. Data Source and Preprocessing. The data used in this research are obtained from the China Shenzhen Government Open Data Platform [40], with a release date of September 21, 2021. The data are in the CSV format and include free-float bike-sharing ID, user ID, borrowing time, returning time, borrowing latitude and longitude, and returning latitude and longitude, as shown in Table 2. Data preprocessing primarily involves removing empty and missing data and eliminating outliers (e.g., latitude and longitude values that significantly deviate from the operating area and ride durations exceeding 6 hours).

The implementation platform is MATLAB R2019a on a notebook with an Intel Core i7-10875H, 2.30 GHz under Windows 10 with 16 GB memory.

To ensure the representativeness, practicality, and portability of the study area, a complex functional area with complete service facilities and high free-float bike-sharing demand is selected for research. The selected area is a rectangular region with latitude ranging from 113.9194 to 113.9394 and longitude ranging from 22.5194 to 22.5294, as shown in Figure 1. The size of the area is approximately 2000 m * 1000 m.

Table 2: Free-float bike-sharing transaction datasheet.

START_TIME	END_TIME	USER_ID	COM_ID	START_LAT	START_LNG	END_LAT	END_LNG
2021/1/30 13:19	2021/1/30 13:23	9fb2d1ec6142ace4d7405b**********	0755**	22.63640929	114.0133089	22.63202908	114.0155348
2021/1/31 23:49	2021/1/31 23:54	1184eecf9f54441b389bcf**********	0755**	22.5854262	113.8589846	22.58103968	113.8577798
2021/1/30 13:09	2021/1/30 13:23	30a457b24805ffab03b9c4**********	0755**	22.64790277	114.0278879	22.63776868	114.0457659
2021/1/30 13:09	2021/1/30 13:20	bee78cd43f65b0ecf3752d**********	0755**	22.51830989	114.0561179	22.52004018	114.0562523
2021/1/31 23:37	2021/1/31 23:59	ced96f24b9754f03e512cf**********	0755**	22.54433607	114.1128739	22.5459811	114.136066
2021/1/30 13:16	2021/1/30 13:23	d283e82de485f692fd2e4a**********	0755**	22.51162231	113.9240799	22.5178703	113.921826

The significance of the asterisk in Table 2 is to hide the user ID (USER_ID) and company ID (COM_ID), mainly to protect the privacy of users and company. The Table 2 main purpose is to introduce the initial style of the data, the initial style of the data in the user ID (USER_ID) and company ID (COM_ID) is with an asterisk, and the user ID (USER_ID) and company ID (COM_ID) data are not used in the later text.

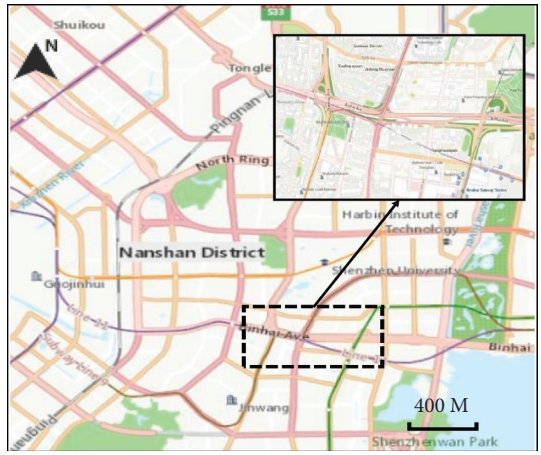

Figure 1: Case study area.

4.2. Free-Float Bike-Sharing Use Characteristics. The weekly borrowing/returning demand for free-float bike-sharing in the study area, as shown in Figure 2, clearly shows that the demand for bikes on weekdays is much higher than that on nonweekdays, and the demand for bicycle use shows obvious bimodal characteristics, reflecting the obvious tidal phenomenon of free-float bike-sharing trips, with the demand in the morning peak being higher than that in the evening peak; on weekdays, the borrowing/returning demand for free-float bike-sharing is similar.

The total number of free-float bike-sharing orders for a week in the study area is 130,507, and the average daily ridership is 18,644. Statistics on the number of orders for a week are shown in Figure 3. The free-float bike-sharing usage on weekdays is more even, and the usage of free-float bike-sharing on weekdays is significantly higher than that on nonworking days, with the highest usage of 20,587 bikes on Wednesday. The number of bikes borrowed and returned at each time on Wednesday is shown in Figure 4, where red represents the demand for returning bikes and black represents the demand for borrowing bikes, showing the tidal phenomenon of bike-sharing use, with obvious morning and evening peaks. From midnight to 5 am, there is a low user demand for bike rides. Starting from 6 am, the demand gradually increases, reaching its peak between 7 am and 9 am, accounting for 48.8% of the total daily usage. The evening peak hours occur between 5 pm and 7 pm, representing 26.3% of the total daily usage. After the evening peak, the bike demand gradually decreases.

In terms of the spatial use characteristics of free-float bike-sharing, first, the region for rasterization, divided into a $20 * 20$ grid, selects the number of bikes borrowing and returning and then calculates the density of free-float bike-sharing in each grid, after visualization as shown in Figure 5. It can be seen that the density of the use of free-floating bike sharing by users in the region is not balanced, with the distribution of bikes in some locations being more concentrated and the distribution of bikes in some locations being more sparse; compared with the free-float bike-sharing borrowing and returning density location area, it can be found that in the same area, the free-float bike-sharing borrowing and returning density is similar.

In the process of selecting and deploying electronic fences for free-float bike-sharing, we believe that it is essential to meet the demand during peak hours. Therefore, we chose the morning peak hours (7 am to 9 am) for our research. We conducted a spatial distribution analysis of free-float bike-sharing during this period and generated origin-destination (OD) kernel density heatmaps, as shown in Figures 6(a) and 6(b). The red areas represent the most frequently utilized regions for free-float bike-sharing usage, while the green areas indicate the least utilized regions. The yellow areas represent transitional zones. It can be observed that the spatial distribution of free-float bike-sharing is highly uneven, with similar intensity in bike returns and borrowings.

4.3. Multiscale Clustering of Electronic Fences. The distribution of free-float bike-sharing in the study area during peak hours is shown in Figure 7, revealing primarily block-shaped, belt-shaped, and point-shaped patterns. The bikes are mainly concentrated along the sides of roads, office buildings, and shopping malls. In this paper, the user's borrowing demand point and returning demand point are considered together, so the borrowing latitude and longitude and returning latitude and longitude data are merged as the location of the user's demand. At the macrolevel, the initial clustering of the data was performed using the K-means algorithm. The evaluation results are presented in Table 3 and Figure 8, showing that the silhouette coefficient is maximized and both the WCSS and CH index exhibit good performance when the data are clustered into six classes. The clustering results, as shown in Figure 9, partition the free-float bike-sharing data within the area into more consistent subsets, which is beneficial for subsequent DBSCAN clustering. This approach enables DBSCAN to adapt to different categories of data and obtain more accurate clustering results.

The DBSCAN clustering method is used at the microlevel. Considering the variability of free-float bike-sharing distribution categories, multiple categories based on *K*-means division are clustered using DBSCAN. We set the

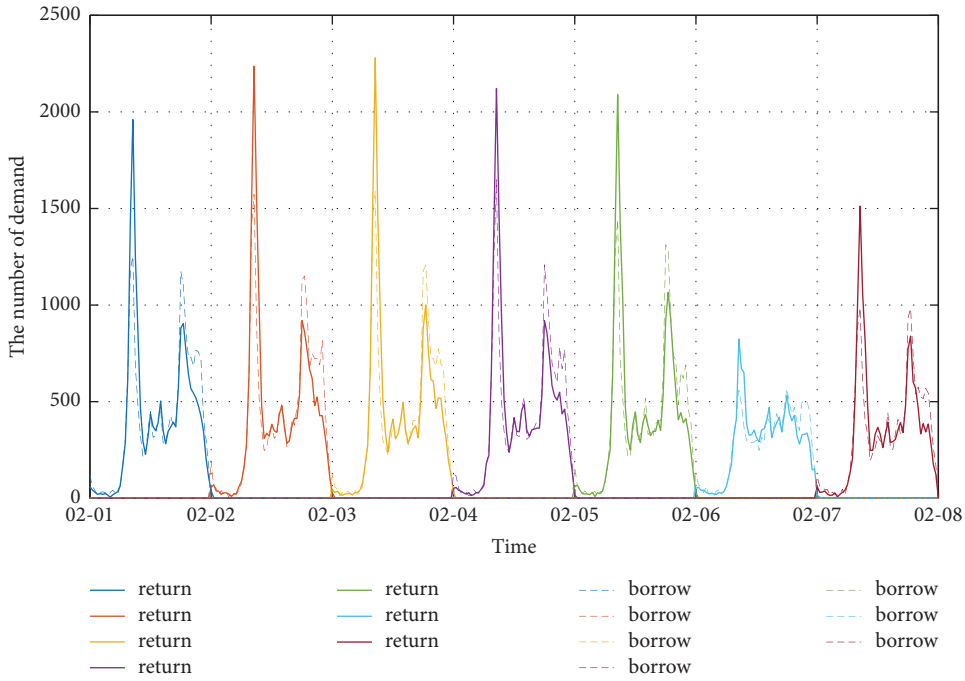

Figure 2: Demand for a week of free-float bike-sharing.

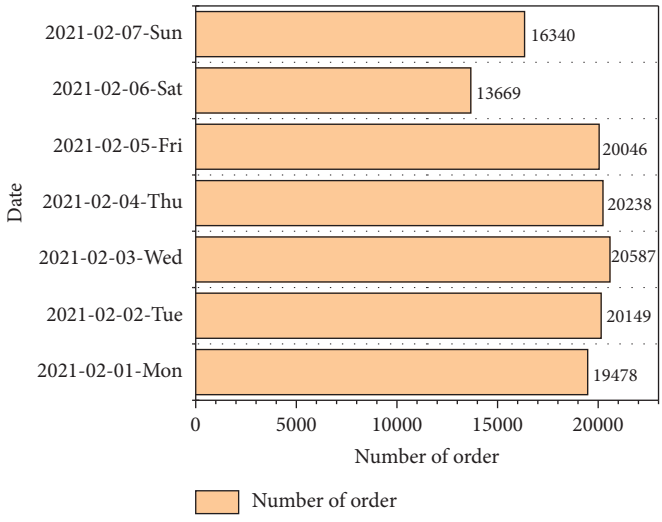

Figure 3: Ridership for a week.

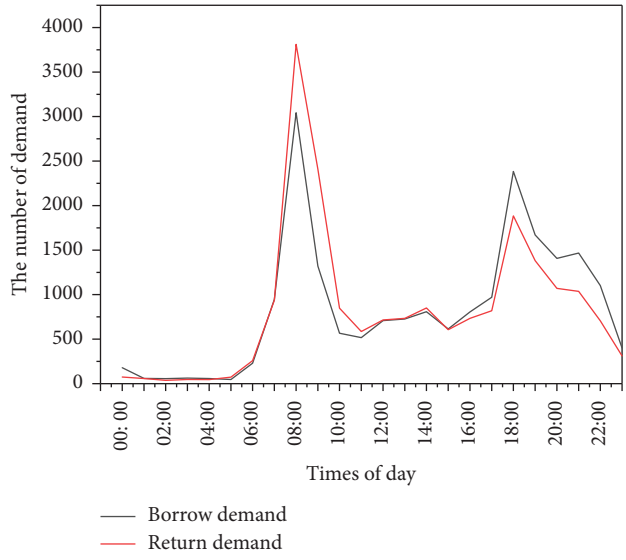

Figure 4: Variation of a daily demand.

minimum neighborhood points (MinPts) to 10 and do not deploy electronic fences if the parking demand is less than 10 bikes. By considering the silhouette coefficient and CH index to evaluate the clustering quality of each category, we focus on capturing the local structure, with the silhouette coefficient chosen as the main evaluation index and the CH index as the auxiliary evaluation index, to select the most appropriate neighborhood radius and enhance the robustness of the results. Figure 10 shows the selection of the neighborhood radius and clustering results for each cluster, where the selection radius of cluster 1 is 24 m, cluster 2 is 16 m, cluster 3 is 17 m, cluster 4 is 20 m, cluster 5 is 25 m, and cluster 6 is 19 m. By doing so, we can more accurately classify the clustering clusters of free-float bike-sharing and improve the results reliability of the clusters.

The results of comparing the multiscale clustering method with direct usage of DBSCAN and *K*-means are presented in Table 4, revealing that the multiscale clustering method demonstrates superior performance across multiple indicators. *K*-means achieves the highest silhouette coefficient when the number of clusters is set to 30. However, the clustering results lack granularity and do

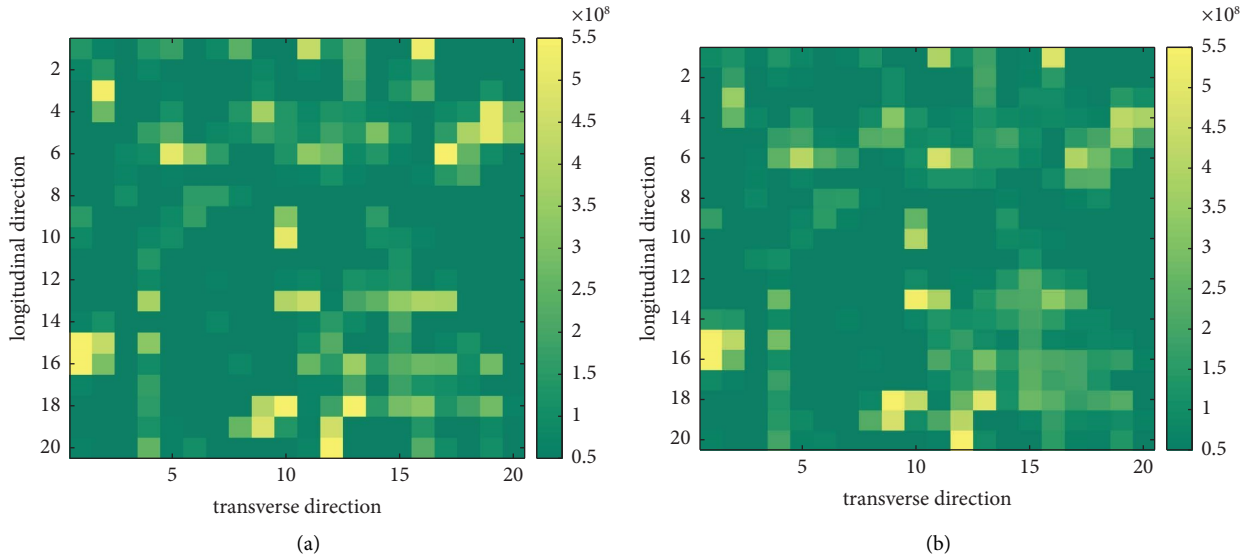

Figure 5: Free-float bike-sharing regional density. (a) Regional borrowing density. (b) Regional returning density.

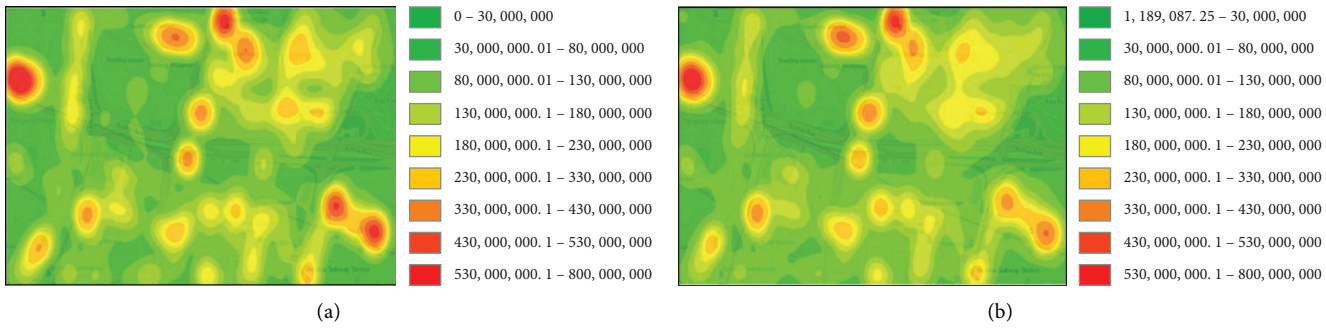

Figure 6: Heat map of demand during peak periods. (a) Heat map of demand for borrowing. (b) Heat map of demand for returning.

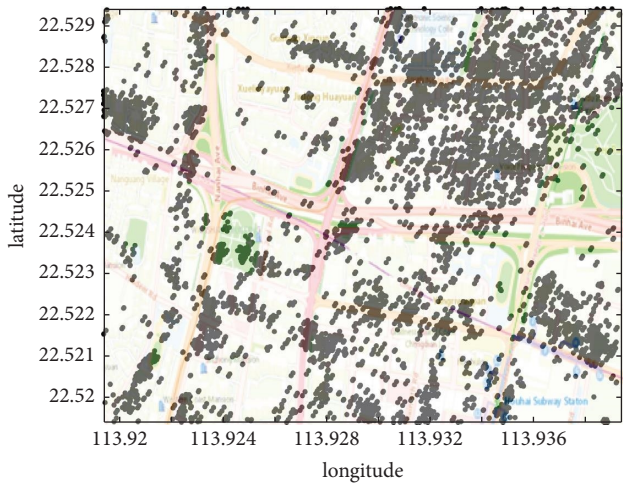

Figure 7: Distribution of bikes in the region.

Table 3: Evaluation of K-means clustering results.

Number of clusters	WCSS	Silhouette coefficient	CH index
2	0.141618843	0.638730861	$2.17E+04$
3	0.093614393	0.570297238	$1.79E+04$
4	0.069217715	0.593869516	$1.52E+04$
5	0.049983302	0.641208203	$1.45E+04$
6	0.035292187	0.668650703	$1.94E+04$
7	0.029886923	0.633170025	$1.82E+04$
8	0.025853272	0.623774029	$1.72E+04$
9	0.022547654	0.629040005	$1.55E+04$
10	0.020072251	0.630456264	1.47E + 04

not produce any noise points. This leads to the establishment of electronic fences around individual free-float bike-sharing, resulting in higher land resource utilization but with low efficiency. In contrast, the multiscale clustering method achieves a balanced level of similarity and dissimilarity between samples, resulting in better clustering outcomes. Furthermore, this method exhibits fewer noise points, indicating that planning the deployment of electronic fences within the clusters can better fulfill user demands. In addition, the multiscale clustering method offers a high computational efficiency, allowing for faster calculations within a shorter timeframe.

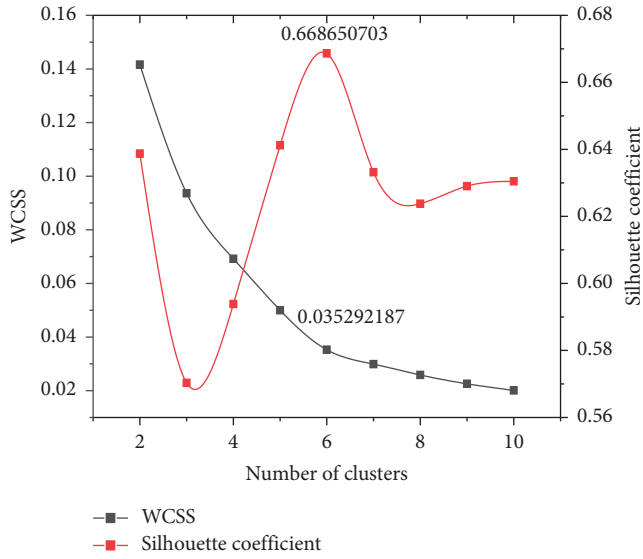

Figure 8: Evaluation of *K*-means clustering results.

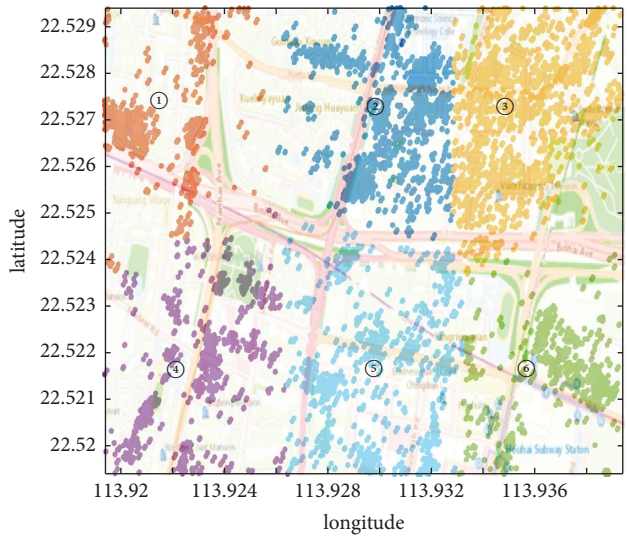

Figure 9: *K*-means clustering results.

4.4. Optimization Model Results. Based on the clustering results, the candidate locations for electronic fences for free-float bike-sharing are determined. The optimization of the number, locations, and capacity of the electronic fences is approached from the perspectives of the enterprise, users, and urban management. The construction cost of an electronic fence [41] is 100 Yuan/place. The cost of land occupation by a bike is 10 yuan/m^2. The user's walking cost [42] is 0.03 yuan/m. The area occupied by a bike is 0.5 m^2/vehicle. The capacity coefficient of the electronic fence is 0.8. The demand location and quantity were obtained by *K*-means clustering. The multiobjective mixed-integer programming model presented in Section 3.2 is solved, and the Pareto solutions are obtained as shown in Figure 11. It can be observed that within the selected area, as the cost of electronic fences (land usage cost and construction cost) increases, the user's walking distance decreases, resulting in increased satisfaction, while the spatial entropy shows an increasing trend.

The grey relational analysis is employed to rank and evaluate the various solutions in the Pareto solution set. The solution with the highest relative grey relational degree is selected as the optimal plan for the deployment of electronic fences. The results are presented in Figure 12, with the optimal ranking of solutions as 4-3-5-6-2-7-8-1-9. Among these solutions, solution 4 is ultimately chosen as the optimal deployment plan for the free-float bike-sharing electronic fences. The construction cost of the electronic fences amounts to 19,418.75 yuan. The average walking distance to access the electronic fences for bike borrowing or returning is 4.31 meters per person. The spatial entropy of the electronic fences is calculated to be 3.1413.

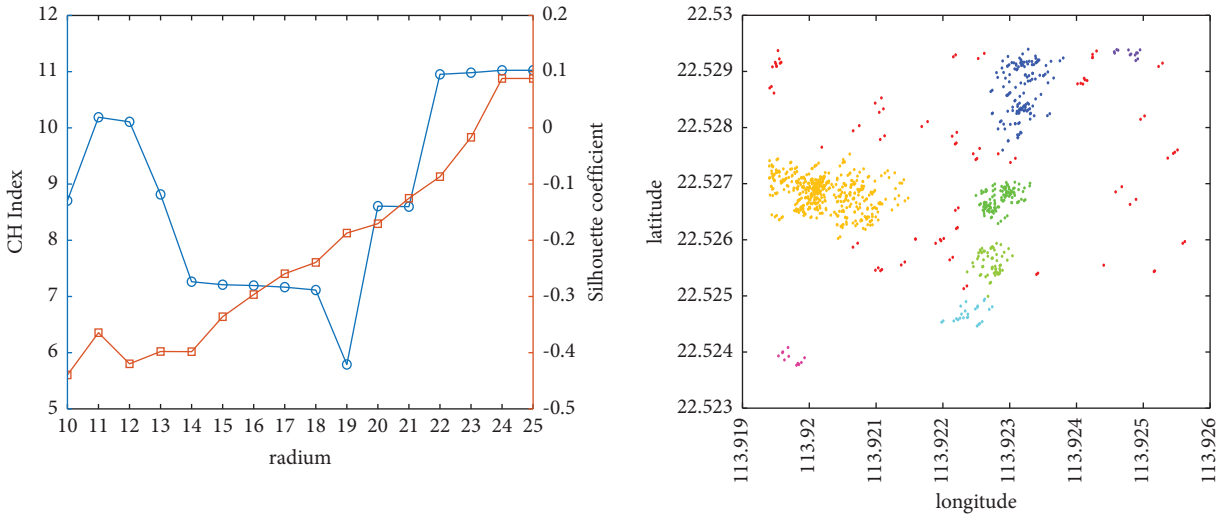

(a)

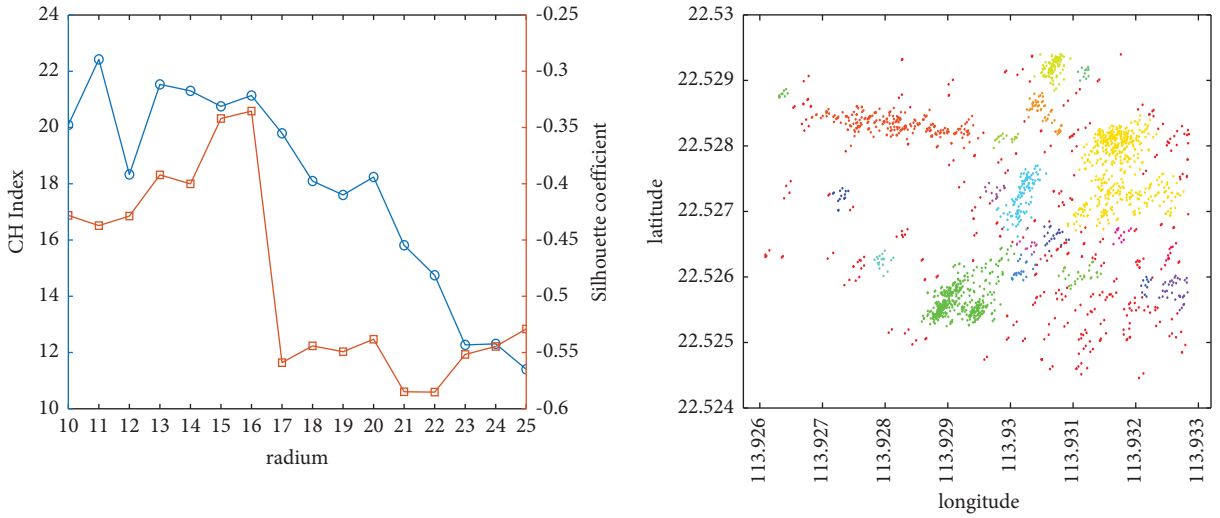

(b)

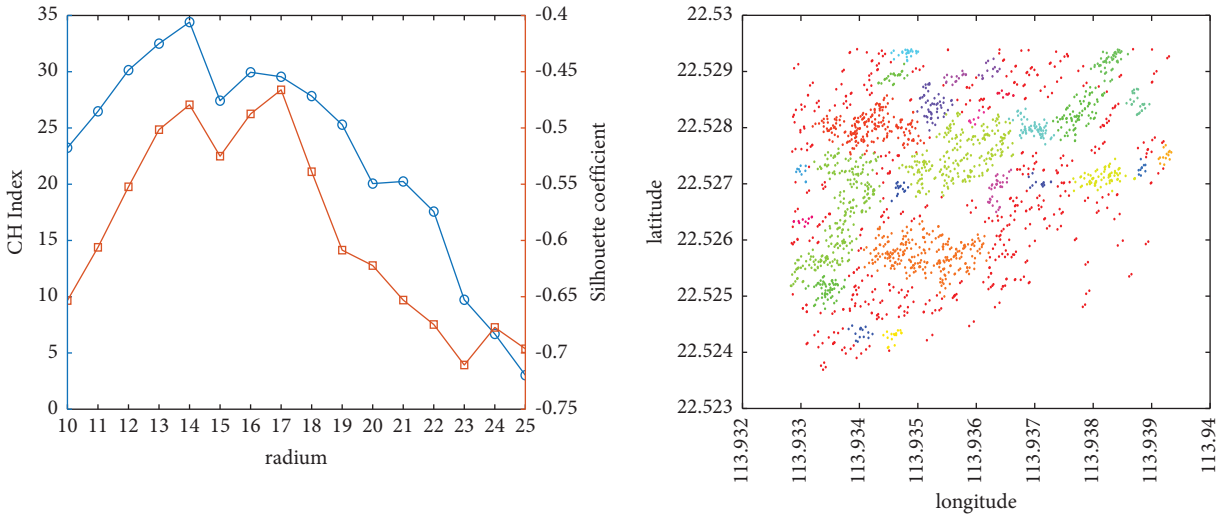

(c)

Figure 10: Continued.

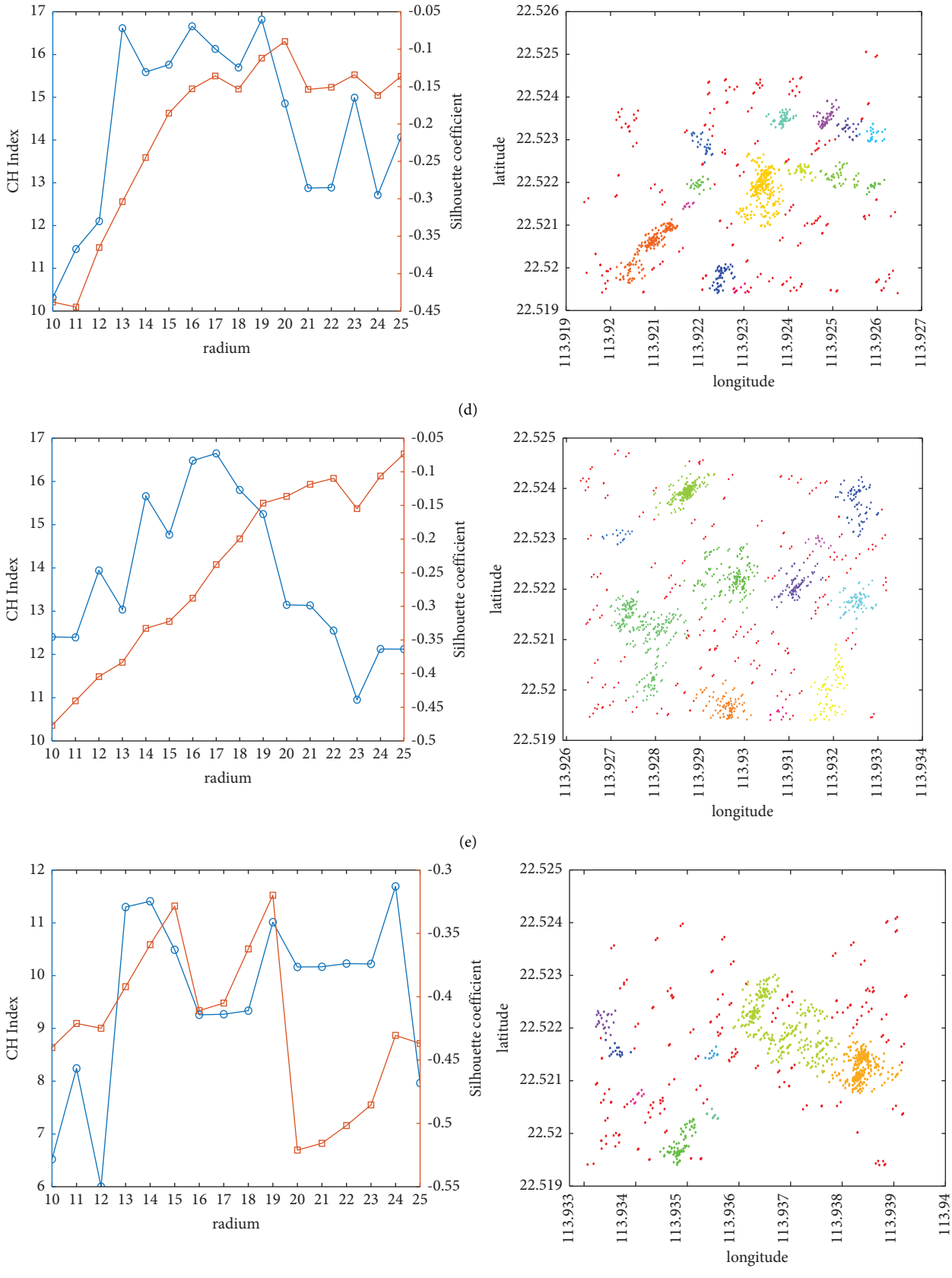

Figure 10: DBSCAN evaluation results. (a) Cluster 1. (b) Cluster 2. (c) Cluster 3. (d) Cluster 4. (e) Cluster 5. (f) Cluster 6.

Table 4: Evaluation of clustering methods.

Clustering methods	Number of clusters	Silhouette coefficient	Noise ratio (%)	Running times (s)
The graded clustering	86	**−0.199433333**	**17.92713179**	**1.25679**
DBSCAN	92	−0.3724	25.11887779	2.3274
K-means clustering	30	0.6418	—	4.0305

The bold values indicate the superiority of the proposed clustering method "the graded clustering" under the three indicators.

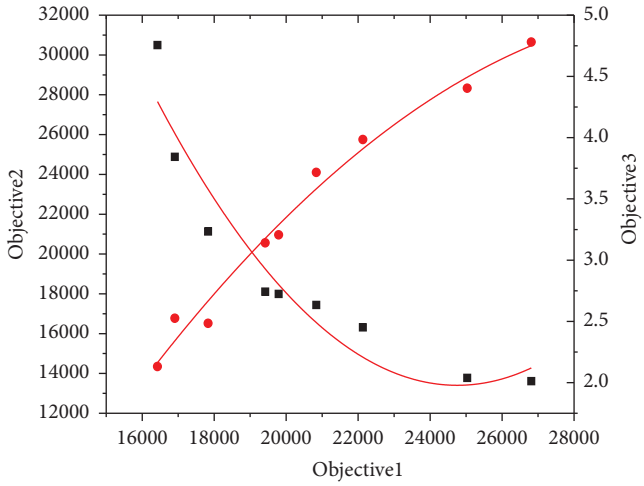

Figure 11: Model Pareto front.

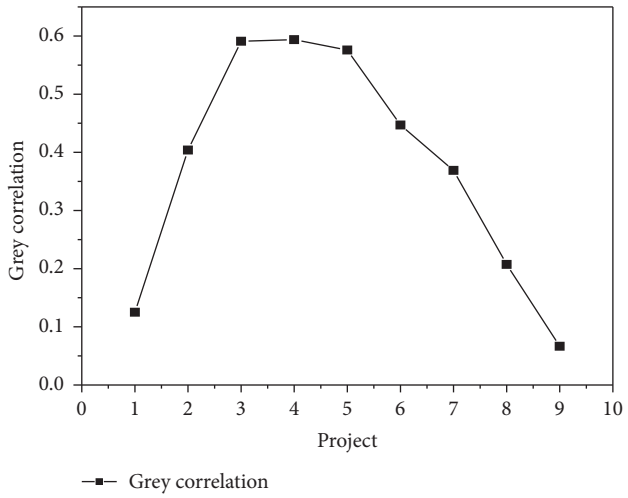

Figure 12: Results of grey correlation analysis.

The specific planning locations and areas of the electronic fences in the research area (1.5 km ∗ 1 km) are presented in Table 5. A total of 25 electronic fences are planned, covering an area of 1691.88 m^2, which accounts for 0.08% of the total area. Users can borrow and return free-float bike-sharing to the suggested nearest e-fence location through the mobile app, as shown in Figures 13(a) and 13(b), where red rectangles and triangles denote the user's borrowing and returning locations, respectively, and the red teardrop shape denotes the location where the e-fence is planned to be deployed. After optimization, the construction cost of the electronic fences decreased by 62% compared to the pre-optimized state. The occupied area has been reduced by 2580 m^2. The spatial entropy of the electronic fences has decreased from 5.4589 to 3.1413, as shown in Figure 14.

Table 5: Electronic fence planning location and area.

Geofence ID	LNG	Lag	Size
1	113.9281603	22.5283309	5.00
2	113.9317266	22.5276928	24.38
3	113.9291724	22.5256362	93.75
4	113.9301945	22.5272407	5.00
5	113.9202352	22.5268393	5.00
6	113.9223946	22.5246752	5.00
7	113.9231791	22.5286652	5.00
8	113.9392356	22.5275044	268.13
9	113.9345844	22.5242855	10.00
10	113.9348061	22.5293223	140.00
11	113.9330447	22.5263384	580.00
12	113.9209068	22.5205277	5.00
13	113.9251718	22.5221308	5.00
14	113.9220825	22.5228825	5.00
15	113.9224973	22.5198016	5.00
16	113.9253612	22.5232444	5.00
17	113.9383767	22.5212525	5.00
18	113.9367847	22.5220752	5.00
19	113.9348579	22.5197727	5.00
20	113.9295770	22.5196784	46.25
21	113.9319384	22.5200114	9.38
22	113.9286964	22.5239334	105.00
23	113.9277341	22.5211274	57.50
24	113.9325372	22.5237139	163.12
25	113.9311444	22.5220788	129.38
Sum			1691.88

5. Discussion

This paper studies the planning and deployment of electronic fences for free-float bike-sharing. Considering the variations in the distribution of free-float bike-sharing parking locations, we utilize large-scale free-float bike-sharing data. At the macrolevel, we employ the *K*-means algorithm to cluster the bike data, capturing the distribution characteristics of the bikes. By considering these distribution characteristics, the bike data are categorized into multiple clusters. At the microlevel, we utilize the DBSCAN algorithm to perform more refined clustering based on the specific distribution features of each bike cluster. By integrating these clustering results, we obtain candidate locations for the electronic fences of free-float bike-sharing. Moreover, from the perspectives of the enterprise, users, and

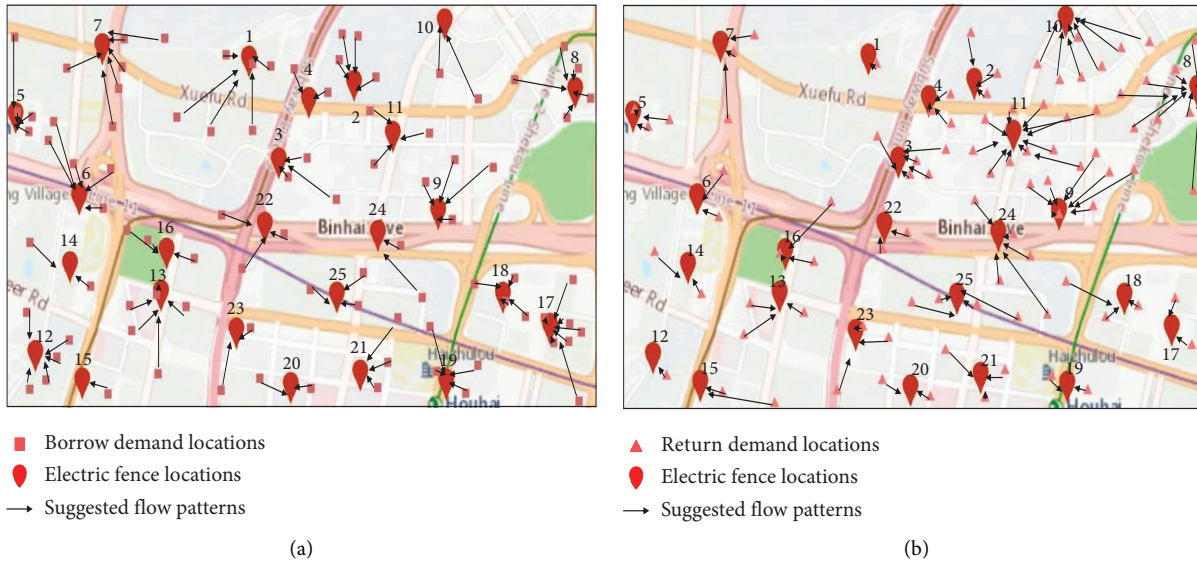

Figure 13: Distribution of demand for (a) borrowing and (b) returning.

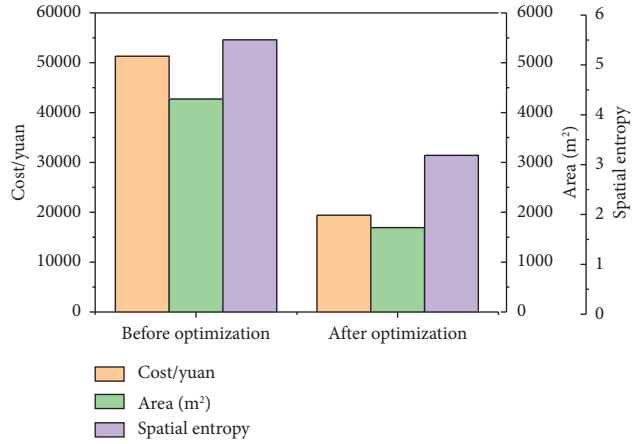

Figure 14: Comparison of indicators before and after optimization.

urban management, we establish a multiobjective site selection model that comprehensively considers factors such as the construction cost of electronic fences, user satisfaction, and the spatial entropy of the fences. Finally, we employ the grey relational analysis to determine the optimal planning and management scheme for the electronic fences.

The spatiotemporal big data of free-float bike-sharing in Shenzhen in 2021 is used as the case study. The experimental results show that compared with the traditional methods using DBSCAN and *K*-means alone, the method proposed in this study is superior in terms of clustering effect, number of noise points, and running time and can achieve a more refined planning for the deployment of electronic fences; through multiscale fusion site selection in the study area of $1.5 * 1$ km, only 25 electronic fences need to be planned and deployed, covering a total area of 1691.88 m^2. This study can provide scientific basis and technical support for the planning and deployment of electronic fences to promote the sustainable development of free-float bike-sharing.

However, there are areas for improvement in this study. In future research, the planning and deployment of electronic fences can be integrated with the scheduling aspect. Considering the tidal phenomenon of free-float bike-sharing, dynamic electronic fences can be implemented. By incorporating land characteristics, the shape of each electronic fence can be refined, making the free-float bike-sharing system more intelligent.

Data Availability

The data used to support the findings of this study have been deposited in the 2021 Shenzhen Government Data Open Platform (https://opendata.sz.gov.cn/).

Conflicts of Interest

The authors declare that they have no conflicts of interest regarding the publication of this paper.

Authors' Contributions

Zhonghua Wei was responsible for funding acquisition and project administration and supervised the study. Houqiang Ma curated the data, performed the formal analysis, proposed the methodology, and wrote the original draft. Yunxuan Li performed the formal analysis, proposed the methodology, provided the software, supervised the study, wrote the original draft, and edited the manuscript.

Acknowledgments

The research was supported by the Natural Science Foundation of Chongqing, China, Grant/Award Number CSTB2022NSCQ-MSX1147.

References

[1] Beijing Transport Institute, "Beijing transport annual Report," 2020, https://www.bjtrc.org.cn.

[2] Y. Wang, Y. Yang, J. Wang, M. Douglas, and D. Su, "Examining the influence of social norms on orderly parking behavior of dockless bike-sharing users," *Transportation Research Part A Policy and Practice*, vol. 147, pp. 284–296, 2021.

[3] S. S. Han, "Co-producing an urban mobility service? The role of actors, policies, and technology in the boom and bust of dockless bike-sharing programmes," *International Journal of Urban Sustainable Development*, vol. 14, no. 1, pp. 209–224, 2022.

[4] W. Wei, Q. Jiang, and C. Gu, "What co-creation countermeasures can users take to stop the disorderly parking of dockless shared bikes?" *Research in Transportation Business & Management*, vol. 43, Article ID 100777, 2022.

[5] Y. Du, F. Deng, and F. Liao, "A model framework for discovering the spatio-temporal usage patterns of public free-floating bike-sharing system," *Transportation Research Part C: Emerging Technologies*, vol. 103, pp. 39–55, 2019.

[6] Y. Yang, A. Heppenstall, A. Turner, and A. Comber, "A spatiotemporal and graph-based analysis of dockless bike-sharing patterns to understand urban flows over the last mile," *Computers, Environment and Urban Systems*, vol. 77, Article ID 101361, 2019.

[7] C. Xu, J. Ji, and P. Liu, "The station-free sharing bike demand forecasting with a deep learning approach and large-scale datasets," *Transportation Research Part C: Emerging Technologies*, vol. 95, pp. 47–60, 2018.

[8] Y. Yang, Y. Yin, Y. Wang, R. Meng, and Z. Yuan, "Modeling of freeway real-time traffic crash risk based on dynamic traffic flow considering temporal effect difference," *Journal of Transportation Engineering, Part A: Systems*, vol. 149, no. 7, 2023.

[9] L. Caggiani, R. Camporeale, M. Ottomanelli, and W. Szeto, "A modeling framework for the dynamic management of free-floating bike-sharing systems," *Transportation Research Part C: Emerging Technologies*, vol. 87, pp. 159–182, 2018.

[10] M. Hua, X. Chen, S. Zheng, L. Cheng, and J. Chen, "Estimating the parking demand of free-floating bike-sharing: a journey-data-based study of Nanjing, China," *Journal of Cleaner Production*, vol. 244, Article ID 118764, 2020.

[11] J. Macqueen, "Some methods for classification and analysis of multivariate observations," *Proceedings of the Symposium on Mathematical Statistics and Probability*, vol. 1, pp. 281–297, 1967.

[12] M. Kryszkiewicz and L. Marzena, "Faster clustering with DBSCAN," in *Proceedings of the Intelligent Information Processing and Web Mining*, Zakopane, Poland, May 2005.

[13] C. Park and S. Y. Sohn, "An optimization approach for the placement of bicycle-sharing stations to reduce short car trips: an application to the city of Seoul," *Transportation Research Part A: Policy and Practice*, vol. 105, pp. 154–166, 2017.

[14] I. Frade and A. Ribeiro, "Bike-sharing stations: a maximal covering location approach," *Transportation Research Part A: Policy and Practice*, vol. 82, pp. 216–227, 2015.

[15] W. El-Assi, M. Salah Mahmoud, and K. Nurul Habib, "Effects of built environment and weather on bike-sharing demand: a station level analysis of commercial bike-sharing in Toronto," *Transportation*, vol. 44, no. 3, pp. 589–613, 2017.

[16] A. Faghih-Imani and N. Eluru, "Incorporating the impact of spatio-temporal interactions on bicycle sharing system demand: a case study of New York CitiBike system," *Journal of Transport Geography*, vol. 54, pp. 218–227, 2016.

[17] Y. Sun, "Sharing and riding: how the dockless bike-sharing scheme in China shapes the city," *Urban Science*, vol. 2, no. 3, pp. 68–115, 2018.

[18] Z. Yuan, X. Yuan, Y. Yang et al., "Greenhouse gas emission analysis and measurement for urban rail transit: a review of research progress and prospects," *Digital Transportation and Safety*, vol. 2, no. 1, pp. 36–51, 2023.

[19] W. Li, S. Wang, X. Zhang, Q. jia, and Y. Tian, "Understanding intra-urban human mobility through an exploratory spatio-temporal analysis of bike-sharing trajectories," *International Journal of Geographical Information Science*, vol. 34, no. 12, pp. 2451–2474, 2020.

[20] Y. Zhang, D. Lin, and Z. Mi, "Electric fence planning for dockless bike-sharing services," *Journal of Cleaner Production*, vol. 206, pp. 383–393, 2019.

[21] T. Guo, J. Yang, L. He, and K. Tang, "Layout optimization of campus bike-sharing parking spots," *Journal of Advanced Transportation*, vol. 2020, Article ID 8894119, 10 pages, 2020.

[22] J. C. García-Palomares, J. Gutiérrez, and M. Latorre, "Optimizing the location of stations in bike-sharing programs: a GIS approach," *Applied Geography*, vol. 35, no. 1-2, pp. 235–246, 2012.

[23] L. M. Martinez, L. Caetano, T. Eiró, and F. Cruz, "An optimisation algorithm to establish the location of stations of a mixed fleet biking system: an application to the city of lisbon," *Procedia- Social and Behavioral Sciences*, vol. 54, pp. 513–524, 2012.

[24] X. Wang, H. Sun, S. Zhang, Y. Lv, and T. Li, "Bike-sharing rebalancing problem with variable demand," *Physica A: Statistical Mechanics and Its Applications*, vol. 591, Article ID 126766, 2022.

[25] V. Mahmoodian, Y. Zhang, and H. Charkhgard, "Hybrid rebalancing with dynamic hubbing for free-floating bike-sharing systems," *International Journal of Transportation Science and Technology*, vol. 11, no. 3, pp. 636–652, 2022.

[26] L. Yang, F. Zhang, M. P. Kwan et al., "Space-time demand cube for spatial-temporal coverage optimization model of shared bicycle system: a study using big bike GPS data," *Journal of Transport Geography*, vol. 88, Article ID 102861, 2020.

[27] Q. Chen and T. Sun, "A model for the layout of bike stations in public bike-sharing systems," *Journal of Advanced Transportation*, vol. 49, no. 8, pp. 884–900, 2015.

[28] Y. Hu, Y. Zhang, D. Lamb, M. Zhang, and P. Jia, "Examining and optimizing the BCycle bike-sharing system – a pilot study in Colorado, US," *Applied Energy*, vol. 247, pp. 1–12, 2019.

[29] R. Guo, X. Luo, C. Wang, and F. He, "Data-driven planning and design for bike-sharing parking spots," *Journal of Transportation Systems Engineering and Information Technology*, vol. 21, pp. 9–16, 2021.

[30] M. Kabak, M. Erbas, C. Cetinkaya, and E. Ozceylan, "A GIS-based MCDM approach for the evaluation of bike-share stations," *Journal of Cleaner Production*, vol. 201, pp. 49–60, 2018.

[31] L. Conrow, A. Murray, and H. Fischer, "An optimization approach for equitable bicycle share station siting," *Journal of Transport Geography*, vol. 69, pp. 163–170, 2018.

[32] P. H. Nyimbili and T. Erden, "GIS-based fuzzy multi-criteria approach for optimal site selection of fire stations in Istanbul, Turkey," *Socio-Economic Planning Sciences*, vol. 71, Article ID 100860, 2020.

[33] S. Banerjee, M. Kabir, N. Khadem, and C. Chavis, "Optimal locations for bikeshare stations: a new GIS based spatial approach," *Transportation Research Interdisciplinary Perspectives*, vol. 4, Article ID 100101, 2020.

[34] Y. Yang, B. Yang, Z. Yuan, R. Meng, and Y. Wang, "Modelling and comparing two modes of sharing parking spots at residential area: real-time and fixed-time allocation," *IET Intelligent Transport Systems*, 2023.

[35] Y. Yang, N. Tian, Y. Wang, and Z. Yuan, "A parallel FP-growth mining algorithm with load balancing constraints for traffic crash data," *International Journal of Computers, Communications & Control*, vol. 17, no. 4, 2022.

[36] C. Fu, N. Zhu, S. Ma, and R. Liu, "A two-stage robust approach to integrated station location and rebalancing vehicle service design in bike-sharing systems," *European Journal of Operational Research*, vol. 298, no. 3, pp. 915–938, 2022.

[37] M. Du, L. Cheng, X. Li, and F. Tang, "Static rebalancing optimization with considering the collection of malfunctioning bikes in free-floating bike-sharing system," *Transportation Research Part E: Logistics and Transportation Review*, vol. 141, Article ID 102012, 2020.

[38] H. Luo, F. Zhao, W. Chen, and H. Cai, "Optimizing bike-sharing systems from the life cycle greenhouse gas emissions perspective," *Transportation Research Part C: Emerging Technologies*, vol. 117, Article ID 102705, 2020.

[39] O. O'Brien, J. Cheshire, and M. Batty, "Mining bicycle sharing data for generating insights into sustainable transport systems," *Journal of Transport Geography*, vol. 34, pp. 262–273, 2014.

[40] Opendata, "Shenzhen government data open platform," 2021, https://opendata.sz.gov.cn.

[41] H. Yang, Y. Zhang, L. Zhong, X. Zhang, and Z. Ling, "Exploring spatial variation of bike-sharing trip production and attraction: a study based on Chicago's Divvy system," *Applied Geography*, vol. 115, Article ID 102130, 2020.

[42] J. Yong, Q. Lu, and J. Li, "Multi-objective bike-sharing electric fence location problem based on robust optimization," *Industrial Engineering & Management*, vol. 28, pp. 151–160, 2023.